Dynamics and Control of the GyrpPTO Wave Energy Point Absorber under Sea Waves

Zhang, Zili; Nielsen, Søren R. K.; Basu, Biswajit

Published in:
Procedia Engineering

DOI (link to publication from Publisher):
10.1016/j.proeng.2017.09.098

Publication date:
2017

Document Version
Publisher's PDF, also known as Version of record

Available online at www.sciencedirect.com

ScienceDirect

Procedia Engineering 199 (2017) 1828–1833

Procedia Engineering

www.elsevier.com/locate/procedia

X International Conference on Structural Dynamics, EURODYN 2017

Dynamics and Control of the GyroPTO Wave Energy Point Absorber under Sea Waves

Zili Zhang[a,*], Søren R.K. Nielsen[b], Biswajit Basu[c]

[a]*Department of Engineering, Aarhus University, 8000 Aarhus, Denmark*
[b]*Department of Civil Engineering, Aalborg University, 9000 Aalborg, Denmark*
[c]*Department of Civil, Structural & Environmental Engineering, School of Engineering, Trinity College Dublin, Dublin 2, Ireland*

Abstract

The Gyroscopic Power Take-Off (GyroPTO) wave energy point absorber has the operational principle somewhat similar to the so-called gyroscopic hand wrist exerciser. Inside the float of GyroPTO, there is a mechanical system made up of a spinning flywheel with its spin axis in rolling contact to a ring. At certain conditions, the ring starts to rotate at a frequency equal to the excitation angular frequency. In this synchronized state, the generator is running at almost constant speed and the generated power becomes constant. In this paper, theoretical modeling of the GyroPTO device is carried out based on analytical rigid body dynamics, and a 3-DOF nonlinear model is established. Simulation results show that synchronization of the device is maintained under harmonic sea wave, but is lost easily under non-harmonic sea waves.To overcome this problem, a magnetic coupling mechanism is added between the spin axis and the flywheel, which also makes semi-active control of the device possible. A 4-DOF model is then established, and simulation results show the introduced magnetic coupling successfully enables synchronization of the device under non-harmonic sea waves.

Peer-review under responsibility of the organizing committee of EURODYN 2017.

Keywords: Gyroscopic power take-off, wave energy convertor, dynamics and control, synchronization

1. Introduction

As an important renewable energy source, wave energy has recently received significant attention in energy and policy agendas. A wave energy converter (WEC) is defined as a dynamic system for converting the energy in waves into mechanical energy stored in the oscillating system. A point absorber is a WEC that is capable of absorbing energy from waves propagating in any direction, and with horizontal dimensions much smaller than the dominating wave length [1]. Different types of point absorber have been proposed, such as the heave absorber [1] and the Wavestar point absorber [2]. The device is typically equipped with an electric power generator via a hydraulic force system. The reaction forces from the hydraulic system are usually used to actively control the motion of the point absorber in

* Corresponding author. Tel.: +4593508334
E-mail address: zili_zhang@eng.au.dk

1877-7058
Peer-review under responsibility of the organizing committee of EURODYN 2017.
10.1016/j.proeng.2017.09.098

such a way that a maximum mechanical energy is supplied to the absorber. With a certain loss due to friction in the actuator, the control forces are then transferred to the generator, where they are converted into electric energy.

For almost all point absorbers, the instantaneous absorbed energy varies significantly with time, making the expensive additional power electronics mandatory before the power can be supplied to the grid. This motivates a search for an alternative device which is able to deliver a more constant power to the grid without introducing power electronics.

The Gyroscopic Power Take-Off (GyroPTO) wave energy point absorber is a possible solution. Its operational principle is somewhat similar to the so-called gyroscopic hand wrist exerciser Powerball [3]. As shown in Fig. 1a, it consists of a float rigidly connected to a lever. In the other end the lever is supported by a hinge (a universal joint), which allows for rotations around a horizontal axis and a vertical axis. Inside the float is a mechanical system made up of a ring, a spinning flywheel and a generator. The ring is free to rotate in a plane orthogonal to the lever, while the spin axis of the flywheel is supported by a track in the ring with a width slightly larger than the diameter of the axis. This track forms a guidance for the precession of the spin axis, which is assumed to roll on the inner side of the track during rotations of the ring without slip. In operational conditions, the wave induced pitch and roll motions of the float produce a time-varying rotation of the ring, which combined with the spinning velocity of the flywheel creates a gyroscopic moment. This moment produces the necessary contact force between the spin axis and the inner side of the track, to provide the friction force making the rolling of the spin axis possible. Therefore, the gyroscopic moment enforces a kinematical constrain between the rotational velocities of the spin axis and the ring. When synchronization of the angular frequency of the ring to the peak frequency of the wave loading takes place, the responses of the ring and the flywheel become almost harmonic. This phenomenon is the basic reason for the functioning of the system. At synchronization, this means that the generated electric power becomes almost constant in time, making the need for additional power electronics unnecessary before the power can be supplied to the grid.

In this paper, the operational principle of the GyroPTO point absorber is explained, and theoretical modeling of the device is performed based on analytical rigid body dynamics. A 3-degree-of-freedom (3-DOF) model is established for the device, which turns out to be highly nonlinear. The wave loading on the float is determined based on the first-order wave theory, where the hydrodynamic coefficients are calculated numerically. It is demonstrated that under monochromatic wave excitations, synchronization of the angular velocity of the ring to the angular wave frequency takes place, and the flywheel is also spinning at a almost constant speed leading to constant power output. However under irregular sea waves, synchronization of the device to the peak frequency of wave is lost. To overcome this problem, an extra magnetic coupling mechanism is introduced between the flywheel and the spin axis. As a result, a 4-DOF model has to be established for the new device. Simulation results show that the introduced coupling mechanism improve the stability (synchronization) of the GyroPTO device significantly in irregular sea waves.

2. Mechanic modeling of the GyroPTO device

Fig. 1 illustrates the schematic details and geometry of the GyroPTO device, of which the float is made up of two semi-spheres (diameter d) connected with a cylindrical part (height c), and the lever has a length of a.

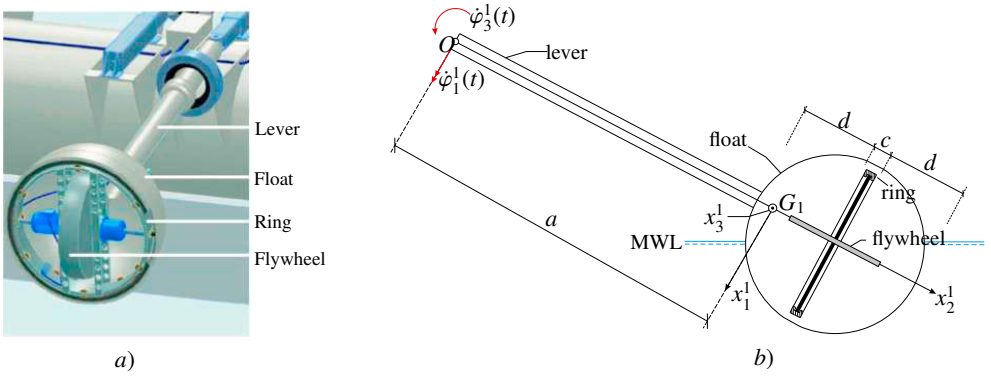

Fig. 1. The GyroPTO point absorber. a) Schematic details. b) Schematic geometry, and definition of the (x_1^1, x_2^1, x_3^1)-coordinate system fixed to the float and lever.

2.1. Kinematic constrain due to the gyroscopic moment

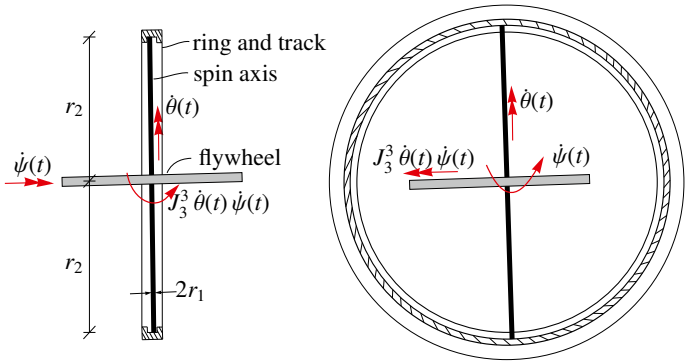

Fig. 2. Rolling contact between the precessing ring and the spinning flywheel due to the gyroscopic moment.

The operational principle of this gyroscopic moment-based device is first explained. As shown in Fig. 2, the spin axis of the flywheel has the radius r_1 and the inner radius of the ring is r_2. The spin axis is supported by a track of the ring with a width slightly larger than $2r_1$. If the ring is set in motion with a rotational velocity $\dot{\psi}(t)$, a gyroscopic moment $J_3^3\,\dot{\theta}(t)\,\dot{\psi}(t)$ on the spinning flywheel is generated according to the law of moment of momentum, where J_3^3 is the mass moment of inertia and $\dot{\theta}(t)$ is the angular spin velocity of the flywheel. This moment produces the necessary contact force between the spin axis and the inner side of the track, providing the friction force to make the rolling of spin axis possible. Therefore, the gyroscopic moment induces a kinematical constrain between the rotational velocities of the spin axis and the ring:

$$\dot{\theta}(t) \;=\; N\,\dot{\psi}(t) \tag{1}$$

where $N = \frac{r_2}{r_1} \gg 1$ is the gear ratio, implying the flywheel is spinning at a much larger speed than the ring.

2.2. Equations of motion of the 3-DOF model

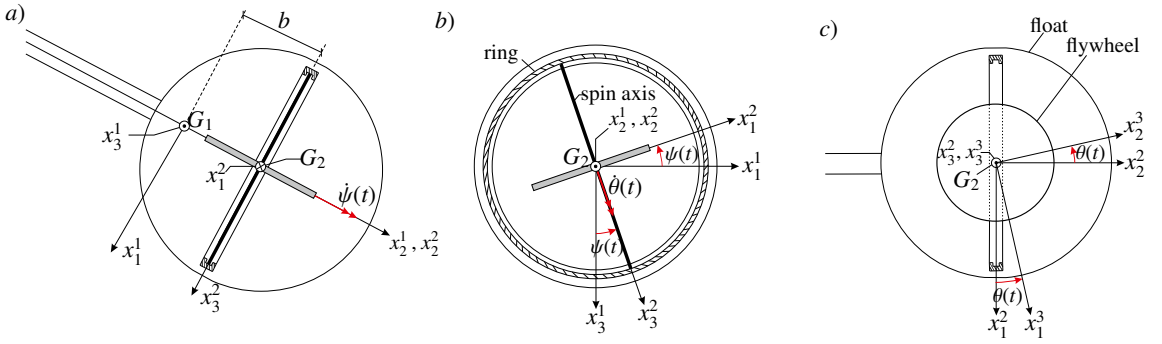

Fig. 3. Definition of the (x_1^2, x_2^2, x_3^2)-coordinate system fixed to the ring.

To derive the equations of motion of the GyroPTO device, three different coordinate systems attached to three rigid bodies moving relative to each other need to be introduced as shown in Fig. 3. Firstly, (x_1^1, x_2^1, x_3^1)- principal axes coordinate system is fixed to the float with origin at G_1, where G_1 is the mass center of gravity of both the lever and the float. Secondly, (x_1^2, x_2^2, x_3^2)- principal axes coordinate system is fixed to the ring with origin at G_2, where G_2 is the center of gravity of both the ring and the flywheel. From Fig. 3a and 3b, it is seen that G_2 is offset from G_1 at a distance of b along the x_2^1-axis, and the x_3^2-axis is rotated from x_3^1-axis with the angle $\psi(t)$ ($\dot{\psi}(t)$ is the rotational velocity of the ring). Thirdly, (x_1^3, x_2^3, x_3^3)- principal axes coordinate system is fixed to the spinning flywheel with its

origin at G_2 as well. The x_1^2- and x_2^2 axes are rotated into the x_1^3- and x_2^3-axes by the rotational angle θ around the x_3^2-axis, where $\dot{\theta}(t)$ is the spinning velocity of the flywheel.

The kinetic energy of the lever and the float T_1, the kinetic energy of the ring T_2, and the kinetic energy of the flywheel T_3 can be formulated in (x_1^1, x_2^1, x_3^1)-, (x_1^2, x_2^2, x_3^2)-, (x_1^3, x_2^3, x_3^3)- coordinate systems, respectively [4]. For example, the kinetic energy of the lever and float T_1 can be written as:

$$T_1 = \frac{1}{2} m_1 \left((\dot{u}_1^1(t))^2 + (\dot{u}_3^1(t))^2 \right) + \frac{1}{2} J_1^1 (\dot{\varphi}_1^1(t))^2 + \frac{1}{2} J_3^1 (\dot{\varphi}_3^1(t))^2 = \frac{1}{2} \left(J_1^1 + m_1 a^2 \right) \left[(\dot{\varphi}_1^1(t))^2 + (\dot{\varphi}_3^1(t))^2 \right] \tag{2}$$

where $\dot{\varphi}_1^1(t)$ and $\dot{\varphi}_3^1(t)$ are the two degrees of freedom describing the rotational velocities of the float in x_1^1- and x_3^1-directions, respectively (as shown in Fig. 1b). $\dot{u}_1^1(t) = -a\dot{\varphi}_3^1(t)$ and $\dot{u}_3^1(t) = a\dot{\varphi}_1^1(t)$ are the translational velocities of the float in x_1^1- and x_3^1- directions. m_1, J_1^1 and J_3^1 are the mass and mass moment of inertias of lever and float, respectively.

Inserting T_1, T_2 and T_3 into Lagrange equation [5], the equations of motion of the GyroPTO can be obtained [4]:

$$\begin{aligned}
&\left(J_1 + J_3 \sin^2\psi \right) \ddot{\varphi}_1^1 + J_3 \sin\psi \cos\psi \, \ddot{\varphi}_3^1 + J_3 \, 2N \sin\psi \, \ddot{\psi} \\
&+ J_3 \left(\sin(2\psi) \, \dot{\varphi}_1^1 + \cos(2\psi) \, \dot{\varphi}_3^1 \right) \dot{\psi} + J_3 \, 2N \cos\psi \, (\dot{\psi})^2 \quad = \sin\psi \, M_g(t) + M_{\varphi_1^1}(t) \\
&J_3 \sin\psi \cos\psi \, \ddot{\varphi}_1^1 + \left(J_1 + J_3 \cos^2\psi \right) \ddot{\varphi}_3^1 + J_3 \, 2N \cos\psi \, \ddot{\psi} \\
&+ J_3 \left(\cos(2\psi) \, \dot{\varphi}_1^1 - \sin(2\psi) \, \dot{\varphi}_3^1 \right) \dot{\psi} - J_3 \, 2N \sin\psi \, (\dot{\psi})^2 \quad = \cos\psi \, M_g(t) + M_{\varphi_3^1}(t) \\
&J_3 \, 2N \sin\psi \, \ddot{\varphi}_1^1 + J_3 \, 2N \cos\psi \, \ddot{\varphi}_3^1 + J_2 \, \ddot{\psi} \\
&- \frac{1}{2} J_3 \left(\sin(2\psi) \left((\dot{\varphi}_1^1)^2 - (\dot{\varphi}_3^1)^2 \right) + 2 \cos(2\psi) \, \dot{\varphi}_1^1 \, \dot{\varphi}_3^1 \right) \quad = -N \, M_g(t)
\end{aligned} \tag{3}$$

where J_1, J_2 and J_3 are quantities related to the mass and geometry properties of the system [4]. $M_{\varphi_1^1}(t)$ and $M_{\varphi_3^1}(t)$ denote the external hydrodynamic moments work conjugated to $\varphi_1^1(t)$ and $\varphi_3^1(t)$ with contributions from quasi-static buoyancy, radiation damping and external wave load [4]. $M_g(t)$ is the generator torque acting on the flywheel. Clearly, $\varphi_1^1(t)$, $\varphi_3^1(t)$ and $\psi(t)$ make up the 3-DOF of the system.

2.3. Performance of the GyroPTO device

Monochromatic (harmonic) wave excitation is first considered with wave period T and amplitude η_0, propagating in the positive x_3^1- direction. As a numerical example, the wave period is chosen to be $T = 2$ s (angular frequency ω=3.14 rad/s) and the amplitude is chosen to be $\eta_0 = 0.1$ m. A reduced-scale model of the GyroPTO is used [4].

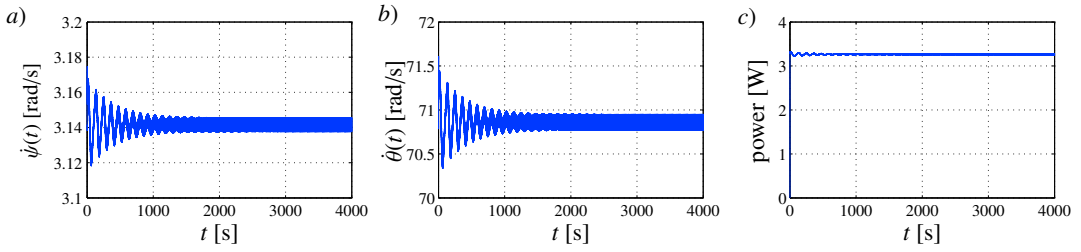

Fig. 4. Rotational velocities of the ring and of the flywheel, and the power output. Harmonic wave excitation, T=2 s (ω=3.14 rad/s), η_0=0.1 m.

Fig. 4a and 4b show the time-series of the rotational velocities of the ring and the flywheel. Synchronization of the device to the harmonic wave excitation is achieved, i.e., the ring is rotating at a constant angular frequency 3.14 rad/s same as the angular frequency of the sea wave, and the flywheel is spinning at a larger (constant) angular frequency 70.82 rad/s due to kinematic constrain. It is also noted that both time-series are not exactly constant, but oscillating around the constant values, resulting from the forced harmonic excitation terms $\sin(2\psi)$ and $\cos(2\psi)$ in Eq. (3c). The power output is illustrated in Fig. 4c, which turns out to be almost constant, as the biggest advantage of this device.

Next, the performance of the GyroPTO device is evaluated under non-harmonic sea waves. Fig. 5 shows the rotational velocities of the ring and flywheel under sea wave which contains two different harmonics. It is seen that

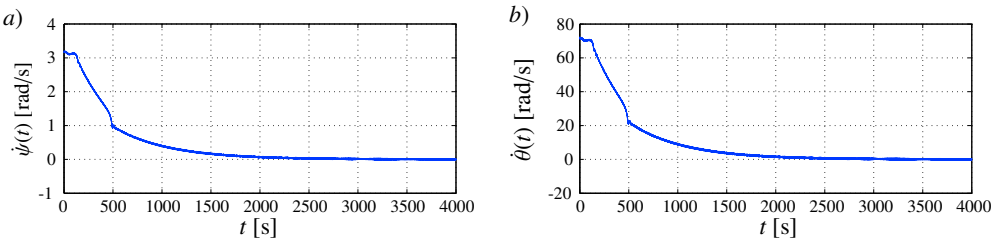

Fig. 5. Rotational velocities of the ring and of the flywheel under sea waves with two harmonics.

synchronization of the device is lost after a short time, i.e., the flywheel spins at a constant velocity 70.82 rad/s for the first 50 s and gradually stops spinning ($\dot{\theta}(t)$ goes to zero) afterwards. Therefore, the GyroPTO device is not performing well under non-harmonic sea waves, and it needs to be technically improved for operating in irregular sea waves.

3. Improved GyroPTO device by introducing a magnetic coupling

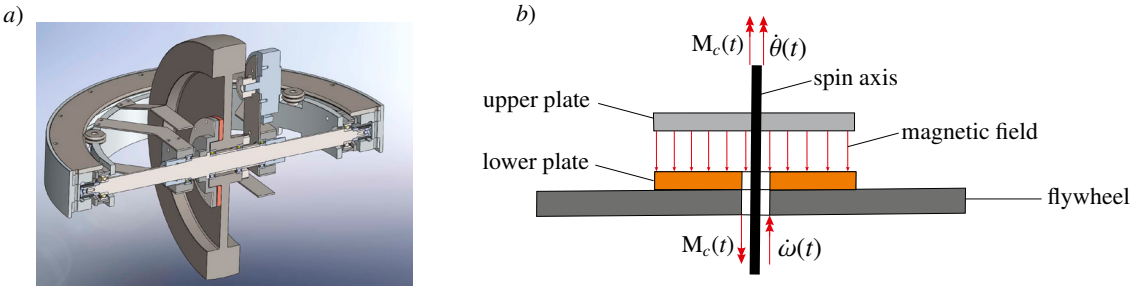

Fig. 6. The magnetic coupling. a) Technical details. b) Schematic principle.

To improve the performance of the GyroPTO device in irregular sea waves, an extra magnetic coupling is introduced between the spin axis and the flywheel, as shown in Fig. 6. Instead of rigidly connected to the flywheel, the spin axis is devised to be connected to the flywheel via a magnetic coupling, which allows for a relative rotation between the spin axis and the flywheel. Two circular discs are fixed to the spin axis and the flywheel, respectively. The flywheel and the lower disc are not in contact with the spin axis, so the spin axis is free to rotate relative to the flywheel. A magnetic field is present between the discs, which produces a torque $M_c(t)$ on the spin axis and the flywheel, the magnitude of which is proportional to the relative rotational velocity of the flywheel with respect to the spin axis, or the so-called slip $\dot{\omega}(t) - \dot{\theta}(t)$:

$$M_c(t) = c_c \left(\dot{\omega}(t) - \dot{\theta}(t)\right) \tag{4}$$

$M_c(t)$ is considered positive when acting in opposite direction of $\dot{\omega}(t)$, as shown in Fig. 6b. Hence, the magnetic coupling acts as a linear viscous damping mechanism on the flywheel. The damping constant c_c depends on the strength of the magnetic field, making semi-active control of this coupling possible. This extra mechanism is expected to reduce the fluctuation of the rotational velocity $\dot{\omega}(t)$, hence stabilizing the synchronization under irregular sea waves.

As a result of the magnetic coupling, a 4-DOF model needs to be established for the new device, $\omega(t)$ representing the rotation of the flywheel, $\psi(t)$ representing the rotation of the ring, $\varphi_1^1(t)$ and $\varphi_3^1(t)$ representing the motions of the float. The procedure of deriving the equations of motion is similar to the 3-DOF model, except that a fourth coordinate system has to be introduced. For brevity, details of the derivation and the final equations of motion will not be given.

Fig. 7 shows the performance of the new GyroPTO device (with magnetic coupling where $c_c = 0.052$ Nms) under the same harmonic sea wave as in Fig. 4. As expected, synchronization is obtained under harmonic wave, which is also the case for the GyroPTO without magnetic coupling. However, it should be noted that the rotational velocities of the ring and flywheel are oscillating around constant values more significantly than the 3-DOF case, due to the fact that the spin axis and the flywheel are not rigidly connected in the new device. This means the introduced magnetic

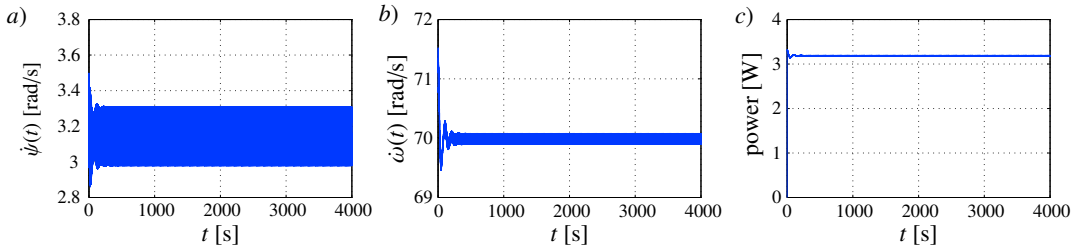

Fig. 7. Rotational velocities of the ring and of the flywheel, and the power output. Magnetic coupling introduced. Harmonic wave excitation, T=2 s (ω=3.14 rad/s), η_0=0.1 m. a) Rotational velocity of the ring. b) Rotational velocity of the flywheel. c) Power output.

coupling actually slightly reduces the performance of the device under harmonic sea wave. But this can be overcome easily by increasing the rigidity of the connection, i.e. by increasing the strength of the magnetic field.

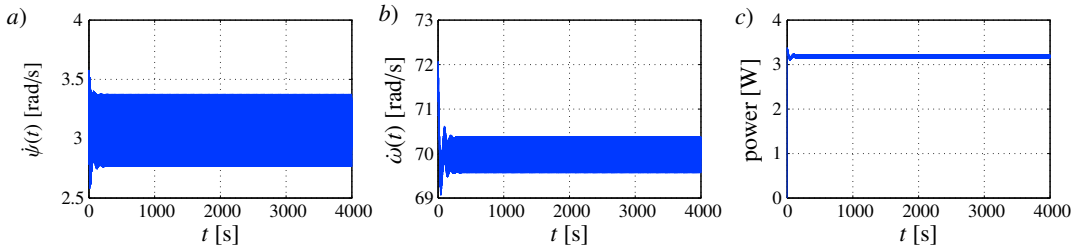

Fig. 8. Rotational velocities of the ring and of the flywheel, and the power output. Magnetic coupling introduced. Sea wave with two harmonics. a) Rotational velocity of the ring. b) Rotational velocity of the flywheel. c) Power output.

More importantly, the performance of the new device under non-harmonic sea wave is illustrated in Fig. 8, where the device is subjected to the same sea wave (containing two harmonics) as in Fig. 5. It is shown that the introduced magnetic coupling successfully enables synchronization of the device under non-harmonic sea wave, which is not the case in Fig. 5. For the new device, both the ring and the flywheel rotate at almost constant velocities, although the oscillations become even larger. Nevertheless, the generated power is around a positive constant value.

4. Conclusions

In this paper, a novel GyroPTO wave energy point absorber is proposed to produce constant power output under sea waves. The gyroscopic moment-based operational principle is explained, and a 3-DOF model of the device is derived based on analytical rigid body dynamics. It is shown that synchronization of the device is obtained under harmonic sea wave, resulting in positive constant power output. However, synchronization is lost very soon under non-harmonic sea waves, i.e. the flywheel stops spinning and the power output becomes zero.

To improve the performance of GyroPTO under irregular sea waves, a magnetic coupling mechanism (linear viscous damping) is introduced between the spin axis and the flywheel, and a 4-DOF model is established for the new device. Simulation results show that the magnetic coupling successfully enables synchronization of the device under non-harmonic sea wave, making the application of this device promising in real sea states.

References

[1] S.R.K. Nielsen, Q. Zhou, M.M. Kramer, B. Basu, Z. Zhang, Optimal control of nonlinear wave energy point converters, Ocean Engineering. 72 (2013) 176–187.
[2] M.T. Sichani, J.B. Chen, M.M. Kramer, S.R.K. Nielsen, Constained optimal stochastic control of non-linear wave energy point converters, Applied Ocean Research. 47 (2014) 255–269.
[3] D.W. Gulick, O.M. O'Reilly, On the dynamics of the dynabee, Journal of Applied Mechanics. 67 (2000) 321–325.
[4] S.R.K. Nielsen, Z. Zhang, M.M. Kramer, J. Olsen, Stability analysis of the Gyroscopic Power Take-Off wave energy point absorber, Journal of Sound and Vibration. 355 (2015) 418–433.
[5] L.A. Pars, A Treatise on Analytical Dynamics, Ox Bow Press, Connecticut, 1979.